The Eleventh International Conference on
Engineering Computational Technology
23–25 August, 2022 | Montpellier, France

Proceedings of the Eleventh International Conference on
Engineering Computational Technology
Edited by B.H.V. Topping and P. Iványi
Civil-Comp Conferences, Volume 2, Paper 5.7
Civil-Comp Press, Edinburgh, United Kingdom, 2022, doi: 10.4203/ccc.2.5.7

Numerical Simulation of Thermal Behaviours in Laser Metal Deposition of Inconel 718

Y.M. Zhang[1], X.W. Yuan[1], W.G. Li[1] and Z.M. Xiao[2]

[1] College of Aerospace Engineering, Chongqing University
Chongqing, China
[2] School of Mechanical and Aerospace Engineering
Nanyang Technological University, Singapore

Abstract

Laser metal deposition (LMD) process is one of the advanced additive manufacturing techniques in which focused energy from a laser beam is used to fuse metallic powders to facilitate them being deposited on the metallic parts at the bottom. The LMD has its uniquely advantageous characteristics, such as small heat-affected zone fabricated, low dilution, and fast repair for metallic components. Although some research efforts has been put on the studies of the process parameters, design of super alloys and mechanical behaviors of components fabricated by the LMD, there is a dire lack of understanding on the thermal behaviours of the melt pool as well as the voids/pores formation during the LMD process. Therefore, in this study a CFD model is developed for the simulation of laser metal deposition of IN718 to investigate the thermal behaviors of melt pool and the potential defects in the clad. Validations on the shape and geometry of the melt pool are made by others' experimental result, indicating that the proposed model is reliable and beneficial in predicting the dynamic behaviour of melt pool and the mass addition in the LMD process. Furthermore, several pores at the bottom of the clad were found in the simulation, it could be due to the absence of wetting behaviour during the solidification of the clad.

Keywords: additive manufacturing, laser metal deposition, melt pool, CFD model, void formation, Solidification.

1 Introduction

Laser metal deposition (LMD) process is an additive manufacturing technique in which focused thermal energy from a laser beam is used to fuse metallic powders to facilitate them being deposited on metallic parts. The LMD has its uniquely advantageous

characteristics, such as small heat-affected zone fabricated, low dilution, and fast repairing for metallic parts [1]. Although some research efforts have been put on the studies of the process parameters, design of super alloys and mechanical behaviours of components fabricated by LMD, there is a dire lack of understanding on the thermal behaviours of the melt pool as well as the void formation during the LMD process. Computational fluid dynamic modelling is widely employed to investigate the formation of melt pool and the flow behaviour of solid-liquid phase during the interaction between the metallic substrate and the laser beam. Meanwhile, in order to accurately capture the free surface of the melt pool, the volume of fluid (VOF) method was introduced [2]. For a steady particle stream, the particles ejected from the nozzle are fused by the laser beam and falling onto the substrate, which is considered as the mass addition in the LMD process, also known as the unique feature of the additive manufacturing [3-5]. And thus, it is of great importance to better understand the evolution of mass addition in the LMD process.

Due to the light weight, large strength and high corrosion resistance [6], nickel-based superalloys are widely used in gas turbines, coal conversion plants and chemical process industries. However, in the manufacturing process of nickel-based superalloy like Inconel 718 (IN718), the controlled solidification is a primary key to achieve superior mechanical properties. Recently, additive manufacturing (AM) with powder bed fusion electron beam shows the promise of pulsed melting scanning patterns to either suppress or promote equiaxed grain formation by controlling local process parameters [7, 8]. However, little research work was found in the solidification of the as-deposited clad in the LMD of IN718, especially in the study of the heat transfer, the metallic flow and the mass addition. Therefore, in this study a computational fluid dynamic (CFD) model is developed for the simulation of laser metal deposition of IN718 to investigate the thermal behaviours of melt pool and the potential defects in the clad during the LMD process.

2 Methods

2.1 CFD model

A CFD model is proposed to study the metallic flow during the LMD process based on the open source-OpenFOAM v3.0.1. The equations for mass conservation and momentum conservation, and energy conservation equation [9]are written as

$$\frac{\partial \bar{\rho}}{\partial t} + \nabla \cdot (\bar{\rho}\vec{u}) = 0, \tag{1}$$

$$\frac{\partial \bar{\rho}\vec{u}}{\partial t} + \nabla \cdot (\bar{\rho}\vec{u}\vec{u}) = -\nabla p + \bar{\rho}g + \nabla \cdot (\bar{\mu}\nabla \vec{u}) + K_0 \frac{(1-\gamma)^2}{\gamma^3 + B_0}\vec{u} + \overrightarrow{f_{st}} + \overrightarrow{f_M}, \tag{2}$$

$$\frac{\partial (\bar{\rho}h)}{\partial t} + \nabla (\bar{\rho}\vec{u}h) = \nabla \cdot (\overline{k / C_p}\nabla h) + Q_{laser} + Q_v + Q_{rad}, \tag{3}$$

where $\bar{\rho}$ is the volume-averaged density, $\vec{u}$ is the vector of velocity, p is the pressure, g is the gravity, $\bar{\mu}$ is the dynamic viscosity, and γ is a temperature-dependent parameter. The fourth term on the right-hand side of Equation (2) is known as Darcy's term employed to indicate the energy dissipation in the mixture of the heat-affected zone. K_0 is the permeability coefficient which is determined by the morphology of porous media. B_0 is a small value in order to avoid division by zero. $\overline{f_{st}}$ and $\overline{f_M}$ represent surface tension force and Marangoni force, respectively. $\bar{k}$ is thermal

conductivity of mixture and $\overline{C_p}$ is specific heat of mixture, Q_{laser} is the heat input irradiated by the laser beam, Q_v is the heat loss by convection and Q_{rad} is the heat loss by radiation. All the details about the parameters can be referred to Ref.[10].

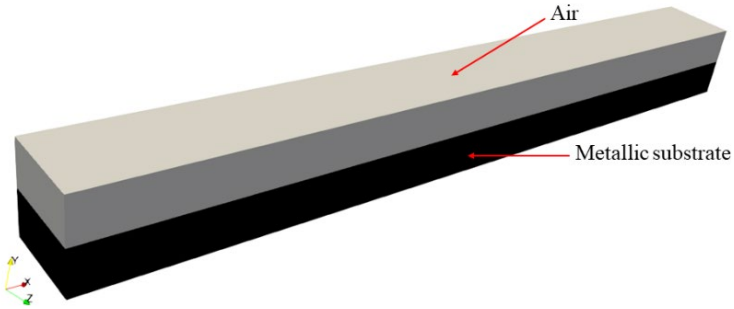

Figure 1: Computational domain for the LMD process.

The 3D computational domain was set to be $20mm \times 6mm \times 6mm$ ($x \times y \times z$), composed of the gaseous region on the top and a cubically metallic substrate with a size of $20mm \times 3mm \times 6mm$, presented in Figure 1. The setting of the boundary conditions in the computational model also can be referred to Ref. [10]. Due to the small melt pool geometry considered, the uniformly sized grid of $0.04 \times 0.04 \times 0.04$ mm^3 was assigned to the computational domain, leading to 1.2 million cells in total. A maximum time step of 1e-3 second was employed to stabilize the simulation.

2.2 Material properties

Commercially available gas atomized IN718 metallic powder was used in this study.

Material property	Symbol	Value
Solid Density at 300 K ($kg \cdot m^{-3}$)	ρ_s	8190
Liquid Density at 1723 K ($kg \cdot m^{-3}$)	ρ_l	7400
Solid specific heat ($m^2 \cdot s^{-2} \cdot K^{-1}$)	C_{ps}	435
Liquid specific heat ($m^2 \cdot s^{-2} \cdot K^{-1}$)	C_{pl}	720
Solidus temperature (K)	T_s	1533
Liquidus temperature (K)	T_l	1609
Thermal conductivity of solid metal ($kg \cdot m \cdot s^{-3} \cdot K^{-1}$)	k_s	8.9
Thermal conductivity of liquid metal ($kg \cdot m \cdot s^{-3} \cdot K^{-1}$)	k_l	29.6
Latent heat of melting ($m^2 \cdot s^{-2}$)	L	2.1e+5
Coefficient of liquid thermal expansion (K^{-1})	β	1.96e-5
Dynamic viscosity ($kg \cdot m^{-1} \cdot s^{-1}$)	μ	0.0056
Stefan-Boltzmann constant ($kg \cdot s^{-3} \cdot K^{-4}$)	σ_s	5.67e-8
Material absorptivity	η	0.2
Emissivity	ε	0.3
Surface tension ($kg \cdot s^{-2}$)	σ	1.82
Surface tension gradient ($kg \cdot s^{-2} \cdot K^{-1}$)	$\frac{d\sigma}{dT}$	-0.37e-3

Table 1: Material properties of IN718 and coefficients used in the simulation.

The average powder particle size was found to be 75 μm and 90% of the particles were within the 60~120 μm range. Table 1 presents the details about the simulation parameters and the values of materials properties based on Ref. [11].

3 Results

The information of the laser beam is given below: the laser power is assumed to be 145 W, the radius of the laser beam with the Gaussian distributed format is 0.125 mm, and the value of the scanning speed is taken as 0.05 m/s.

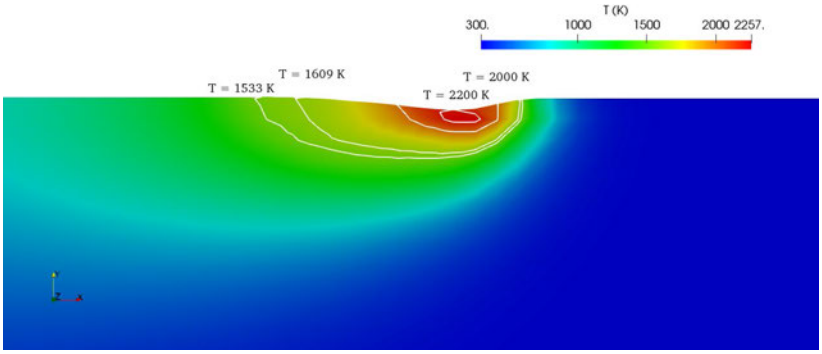

Figure 2: Temperature distribution of the melt pool at the section profile of the *x*-*y* plane.

The temperature distribution of the melt pool, the temperature distribution of the melt pool at the section profile of the *x*-*y* plane (z = 0) is presented in Figure 2, and several temperature contour lines are depicted to explore the thermal behaviour of the melt pool. The solidus temperature and the liquidus temperature are 1533 K and 1609 K, respectively. It is observed that the temperature at the center of melt pool is up to 2250 K, and the top surface of melt pool exhibits to be concaved. One interesting observation is that the highest temperature does occur beneath the top surface rather than the top surface. It could be ascribed by the conduction.

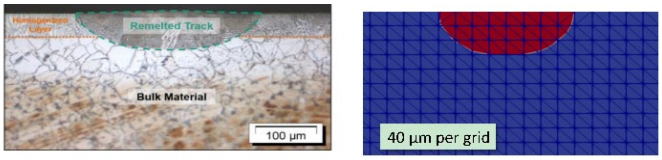

Figure 3: The comparison of the melt pool geometry between the experimental (Ref. [7]) and current numerical results.

Comparison of the melt pool geometry between the experimental result (Ref. [7]) and the numerical results is presented in Figure 3. A good agreement of the melt pool shape is found. As the experimental result was obtained by remelting technique, the width of the melt pool is a little larger than that from the numerical simulation. The minimal deviation within 15 % shows that the current numerical model and the values of the parameters adopted are reasonable and reliable.

The overall clad at the middle section profile (in the *x*-*y* plane with z = 0.0) is presented in Figure 4(a). Overall, the smooth surface of the clad is obtained along the laser scanning direction, except those in the front and the rear of the clad. It is because there is a warm up period at the beginning, and at last the solidification of the clad occurs with high cooling rate. Interestingly, several pores are observed in the clad, shown in Figure 4(b). It is noticed that most of them are located at the bottom of the clad. The possible reason for holes formed in the clad could be due to the lack of fusion. The absence of wetting behaviour therefore introduces the pores or voids in the clad.

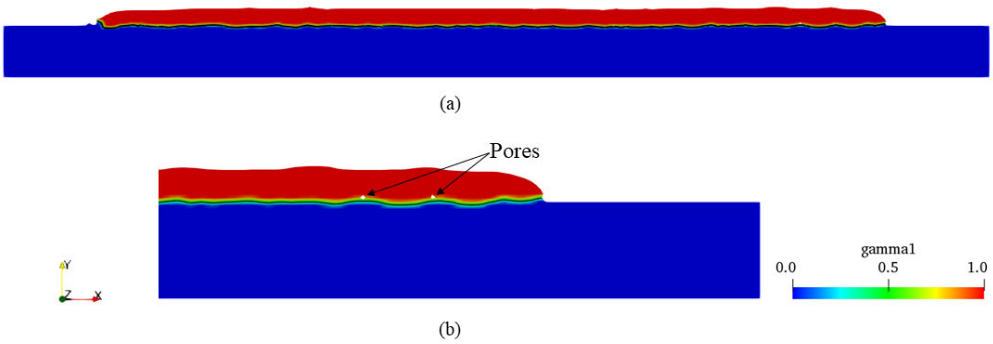

Figure 4: (a) Overall clad at the middle section profile (in the *x*-*y* plane) and (b) One enlarged segments of the clad with two pores.

4 Conclusions and Contributions

In this study a CFD model is proposed to simulate the whole process of laser metal deposition. The physical phenomena related to this process, such as the thermal behaviour, the molten flow and clad formation, are thoroughly investigated. Validations on the shape and geometry of the melt pool are made, indicating that the proposed model is reliable and beneficial in predicting the dynamic behaviours of melt pool and the mass addition in the LMD process. Based on the temperature distribution of the melt pool, it is observed that the temperature at the center of melt pool is up to 2250 K, and the top surface of melt pool exhibits to be concaved. Moreover, several holes found in the simulation could be due to the lack of fusion. At the bottom the energy may be inadequate to fully melt the solidius substrate which the melted particles tend to merge together rather than spread onto. The absence of wetting behaviour therefore introduces the pores or voids during the solidification of the clad. The influences of the significant process parameters such as the laser power, the scanning speed and the powder mass flow rate on the clad, especially on the mechanism of void formation will be investigated in the future work.

Acknowledgements

This work was financially supported by the Fundamental Research Funds for the Central Universities (Project No. 2021CDJQY-056) and Science and Technology Research Program of Chongqing Municipal Education Commission (Project No. KJCXZD2020002).

References

[1] E. Toyserkani, S. Corbin, and A. Khajepour, *Laser Cladding*. Canada: CRC, 2005.

[2] C. Tang, J. L. Tan, and C. H. Wong, "A numerical investigation on the physical mechanisms of single track defects in selective laser melting," *International Journal of Heat and Mass Transfer,* Article vol. 126, pp. 957-968, 2018, doi: 10.1016/j.ijheatmasstransfer.2018.06.073.

[3] J. Ibarra-Medina, "Development and application of a cfd model of laser metal deposition," PhD School of Mechanical, Aerospace and Civil Engineering, University of Manchester, 2012.

[4] I. Tabernero, A. Lamikiz, S. Martínez, E. Ukar, and L. N. L. D. Lacalle, "Geometric Modelling of Added Layers by Coaxial Laser Cladding," in *Physics Procedia*, 2012, vol. 39, pp. 913-920, doi: 10.1016/j.phpro.2012.10.116.

[5] J. I. Arrizubieta, A. Lamikiz, F. Klocke, S. Martínez, K. Arntz, and E. Ukar, "Evaluation of the relevance of melt pool dynamics in Laser Material Deposition process modeling," *International Journal of Heat and Mass Transfer,* vol. 115, pp. 80-91, 2017,

doi: 10.1016/j.ijheatmasstransfer.2017.07.011.
[6] A. Ramakrishnan and G. P. Dinda, "Direct laser metal deposition of Inconel 738," *Materials Science and Engineering: A,* vol. 740-741, pp. 1-13, 2019, doi: 10.1016/j.msea.2018.10.020.
[7] A. Temmler, T. Schmickler, and E. Willenborg, "Surface Structuring by laser remelting of Inconel 718," presented at the Lasers in Manufacturing Conference, Aachen, Germany, 2015.
[8] Y. S. Lee and W. Zhang, "Modeling of heat transfer, fluid flow and solidification microstructure of nickel-base superalloy fabricated by laser powder bed fusion," *Additive Manufacturing,* vol. 12, pp. 178-188, 2016, doi: 10.1016/j.addma.2016.05.003.
[9] C. Panwisawas, C. Qiu, M. J. Anderson, Y. Sovani, R. P. Turner, M. M. Attallah, J. W. Brooks and H. C. Basoalto, "Mesoscale modelling of selective laser melting: Thermal fluid dynamics and microstructural evolution," *Computational Materials Science,* vol. 126, pp. 479-490, 2017, doi: 10.1016/j.commatsci.2016.10.011.
[10] Y. M. Zhang, C. W. J. Lim, C. Tang, and B. Li, "Numerical investigation on heat transfer of melt pool and clad generation in directed energy deposition of stainless steel," *International Journal of Thermal Sciences,* vol. 165, 2021, doi: 10.1016/j.ijthermalsci.2021.106954.
[11] G. L. Knapp, N. Raghavan, A. Plotkowski, and T. DebRoy, "Experiments and simulations on solidification microstructure for Inconel 718 in powder bed fusion electron beam additive manufacturing," *Additive Manufacturing,* vol. 25, pp. 511-521, 2019, doi: 10.1016/j.addma.2018.12.001.